SUPPLEMENTAL MATERIAL I: SEM IMAGE OF PHOTONIC CRYSTAL RESONATOR

Figure S1 below is a scanning electronic microscopy image of a typical evanescently coupled photonic crystal resonator used in these experiments.

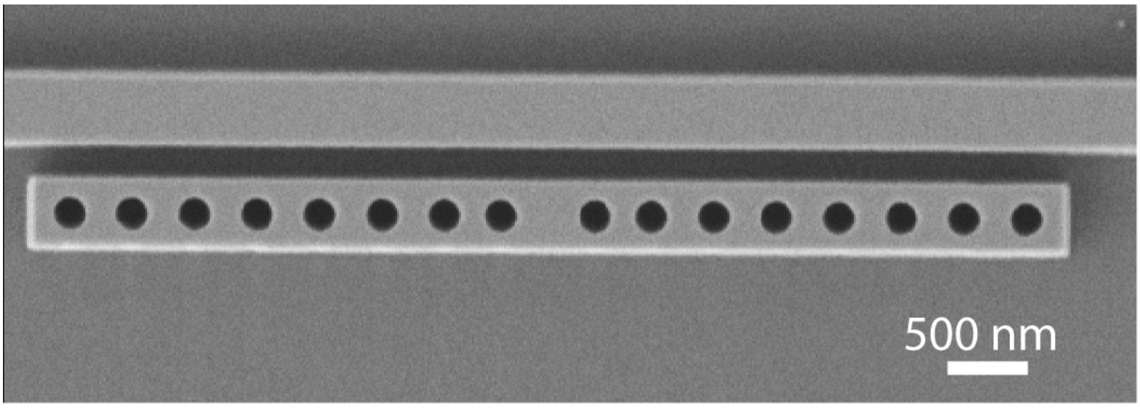

Figure S1: SEM Image of photonic crystal resonator. The photonic crystal resonators used in this work were fabricated from Silicon-on-Insulator using electron-beam lithography fabrication techniques as described in Supplemenal Material II.

SUPPLEMENTAL MATERIAL II: METHODS SUMMARY

The devices used here (See Supplementary information section I for an SEM image) were fabricated from Silicon-on-Insulator wafers having a device thickness of 250 nm. XR-1541 electron beam resist (HSQ, Dow-Corning Corporation) was spun on the wafer and the devices were patterned using a Leica VB6-HR electron beam lithography system. Details regarding the fabrication procedure of these devices have been outlined previously[1] with one notable difference: the use of e-beam evaporated silicon oxide as the nanotaper cladding in place of SU-8. A tunable infrared laser was connected to a tapered fibre lens via an erbium-doped-fibre-amplifier (EDFA) to produce enough optical power for performing these trapping experiments. Fluorescent polystyrene nanoparticles with diameters ranging from 50-500 nm (Duke Scientific) and refractive index 1.59 were mixed in a 100mM phosphate buffer solution. 1% Triton X-100 surfactant was added to minimize adhesion and stiction issues between the polystyrene nanoparticles, microfluidic channel surfaces as well as the substrate of the chip.

PDMS microfluidic channels were bonded to the chips after plasma treatment for 15 seconds. The channels were 120 μm wide and 5 μm tall. A syringe pump was used to control the fluid flow within the microfluidic channels. Measurements of the particle position and Brownian motion were made using the Video Spot Tracker software package.

SUPPLEMENTAL MATERIAL III: SUPPRESSED BROWNIAN MOTION AND TRAPPING STIFFNESS MEASUREMENT

In this article, we estimate the radial trapping stiffness of our resonant optical trap by analyzing the suppressed Brownian motion of a trapped 200-nm polystyrene nanoparticle when the power at the output of the waveguide was measured to be 175 µW. For a particle in a harmonic potential with stiffness k_x, the equipartition theorem states that[2]:

$$\frac{1}{2}k_b T = \frac{1}{2}k_x \left\langle x^2 \right\rangle \tag{1}$$

where k_B is the Boltzmann constant, T is the absolute temperature and $\left\langle x^2 \right\rangle$ is the positional variance of the trapped particle. By measuring the instantaneous position of the particle, it is possible to determine the stiffness of the optical trap. However, detection systems such as video cameras do not measure the instantaneous particle position. Instead, they introduce a bias in the measurements due to the finite integration time W of the device. Wong *et al.*[3] performed a detailed experimental and theoretical analysis to demonstrate a novel method that accounts for these systematic biases introduced in measurements due to video-image motion blur. The true and measured variance var(X) and var(X_{meas}) are related by[3-4]:

$$\operatorname{var}\left(X_{meas}\right) = \operatorname{var}\left(X\right) S\left(\alpha\right) \tag{2}$$

where $S\left(\alpha\right)$ is the motion blur correction function. α is given by $Wk_x / 2\pi\gamma$ where γ is the Stoke's drag coefficient and W is 51.17 ms. By combining Eqs. (1) and (2) we obtain:

$$\operatorname{var}\left(X_{meas}\right) = \frac{\left(k_B T\right) W}{2\pi\gamma}\left[\frac{S\left(\alpha\right)}{\alpha}\right] \tag{3}$$

We solve Eq. (3) numerically for α using values for $\operatorname{var}(X_{meas})$ and $\operatorname{var}(Y_{meas})$ determined from Fig. 5. Thus we obtain trap stiffness values along the *X* and *Y* axes of 3.73×10^{-3} pN/nm and 3.50×10^{-3} pN/nm respectively. We also determine the true standard deviation of the Brownian fluctuations in the *X* and *Y* axes to be 33.2 nm and 34.3 nm respectively.

The resonant output spectrum for the photonic crystal resonator was recorded. The ratio of the output power at the resonant wavelength to the output power for a non-resonant wavelength was determined to be 0.44. Additionally, silicon waveguides that are fabricated using HSQ/XR-1541 (Dow-Corning Corporation) typically exhibit propagation losses around 2 dB/cm[5]. Taking these into account, we estimate the corresponding input power in the waveguide to be 630.4 μW. Thus, the power normalized stiffness for our resonant optical trap is determined to be 5.90 pN nm^{-1} W^{-1} and 5.55 pN nm^{-1} W^{-1} along the *X* and *Y* axes respectively thus giving us a final radial trap stiffness of 2.86 pN nm^{-1} W^{-1}.

By performing a detailed three dimensional finite element numerical analysis we obtain theoretical trap stiffness values of 15.85 pN nm^{-1} W^{-1} (X-axis) and 8.14 pN nm^{-1} W^{-1} (Y-axis) resulting in a net radial trap stiffness of 5.38 pN nm^{-1} W^{-1}. The results of these calculations are shown in Figure S2.

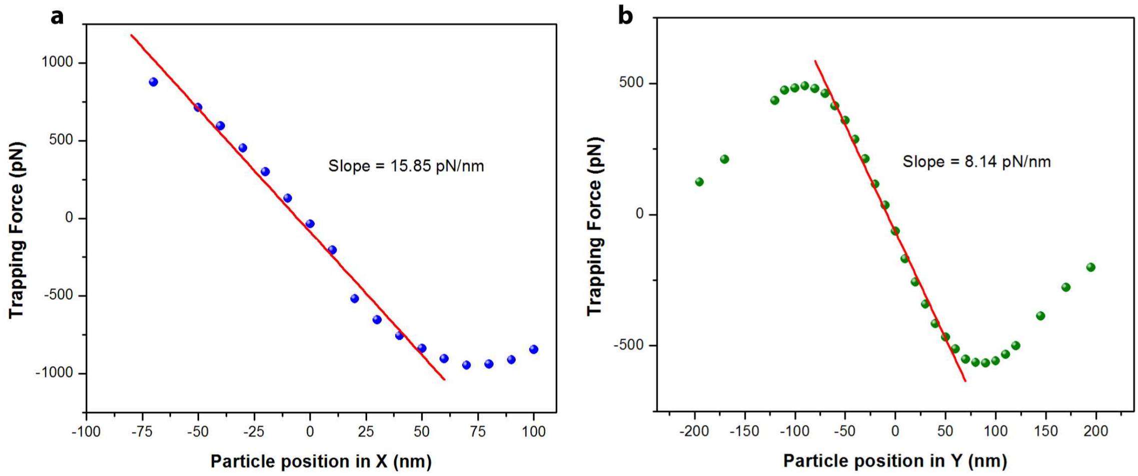

Figure S2: Numerical analysis of trapping stiffness for 200-nm polystyrene nanoparticles. All Forces are normalized to 1-W of input power in the waveguide. **(a)** Force experienced by a 200-nm trapped polystyrene nanoparticle as it is displaced along the length of the resonator (X-axis). The zero X-axis value corresponds to the stable trapping position at the lobe centre. The slope in the linear region of the plot indicates a trapping stiffness of 15.85 pN nm^{-1} W^{-1} along the X-axis. **(b)** Graph illustrating the restoring force on a 200-nm particle as it is displaced in the Y-axis, normal to the length of the resonator. The zero Y-axis value corresponds to the stable trapping position at the lobe centre. The slope of the linear region in the plot indicates a trapping stiffness of 8.14 pN nm^{-1} W^{-1} along the Y-axis.

REFERENCES

1. Mandal, S.; Erickson, D. *Opt. Express* **2008,** 16, 1623-1631.
2. Neuman, K. C.; Block, S. M. *Rev. Sci. Instrum.* **2004,** 75, 2787-2809.
3. Wong, W. P.; Halvorsen, K. *Opt. Express* **2006,** 14, 12517-12531.
4. Schonbrun, E.; Rinzler, C.; Crozier, K. B. *Appl. Phys. Lett.* **2008,** 92, 071112-3.
5. Xiao, S.; Khan, M. H.; Shen, H.; Qi, M. *Opt. Express* **2007,** 15, 14467-14475.